

Figures

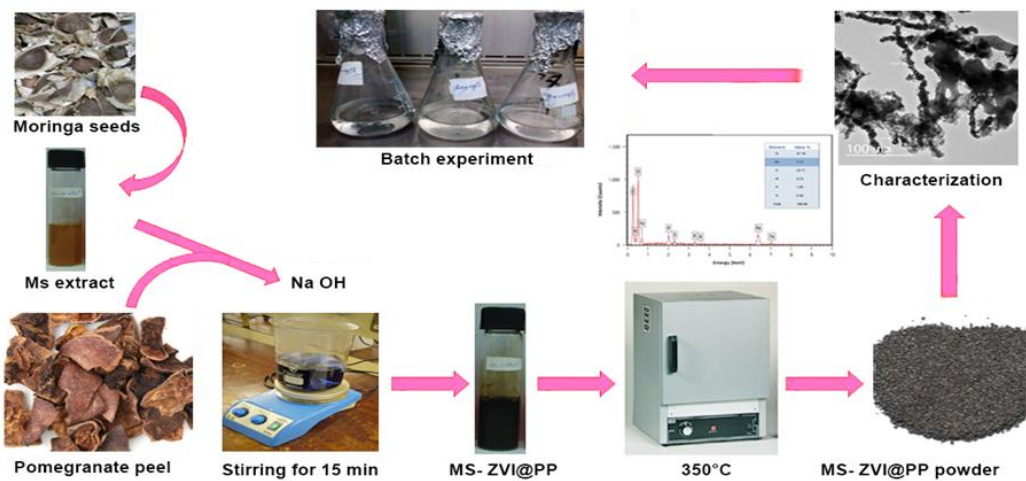


Figure 1. Schematic diagram for the Green Synthesis of nZVI using MO seed extract with incorporate pomegranate peel powder.

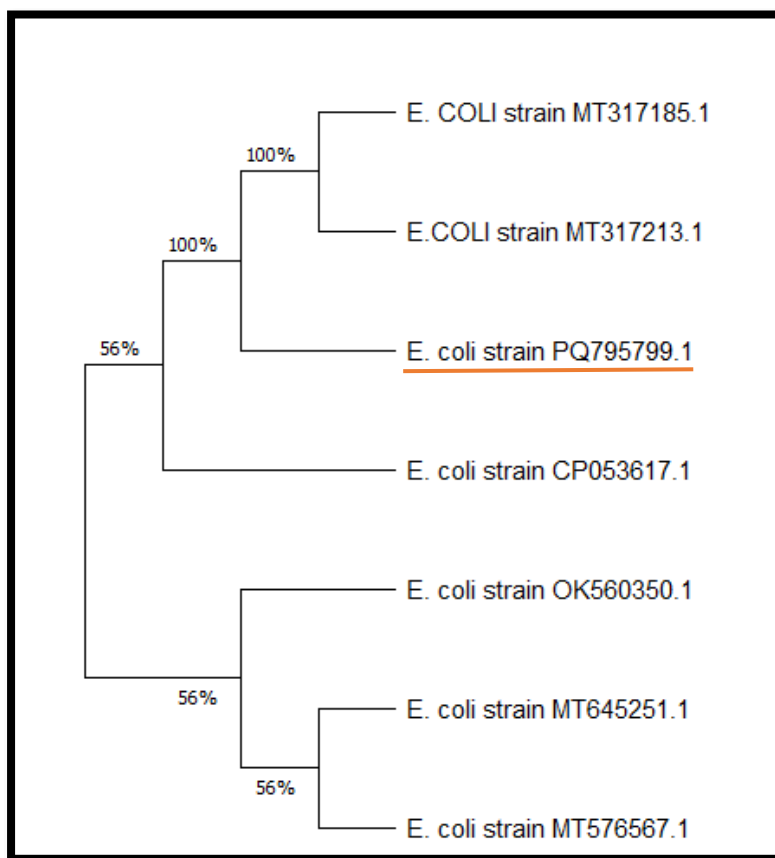
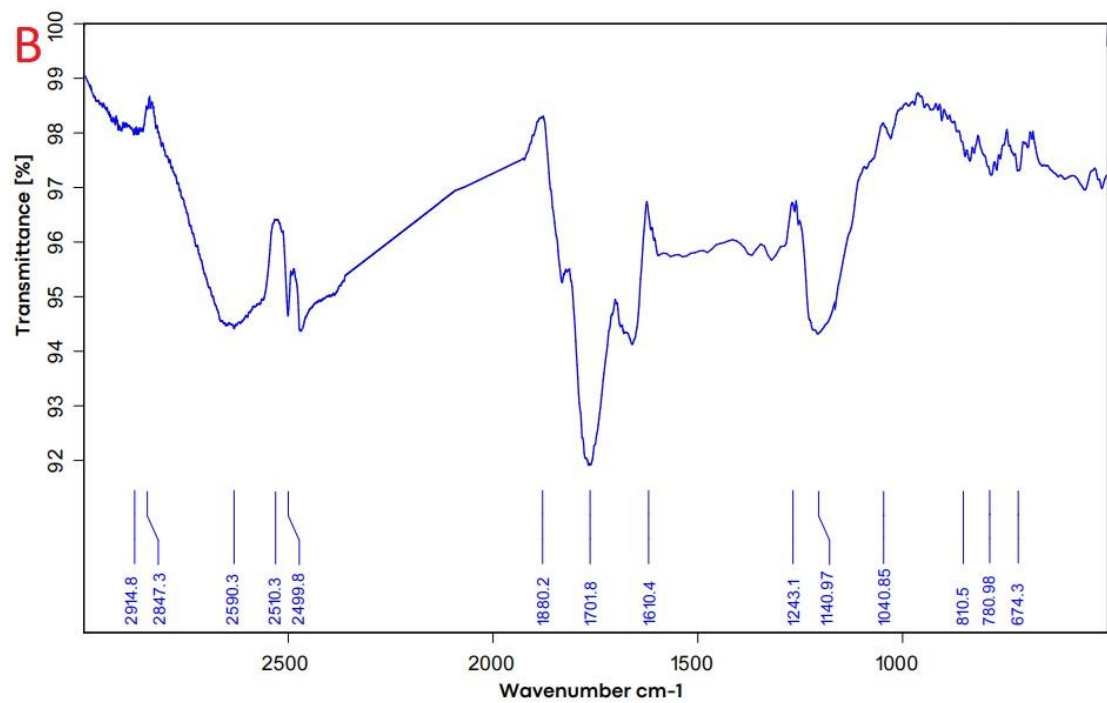
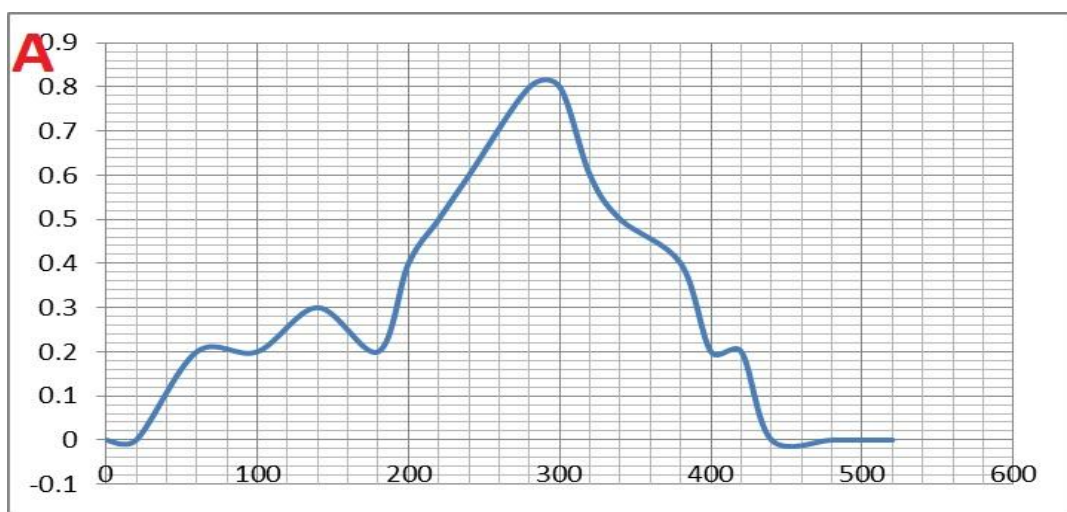


Figure 2 | Phylogenetic tree derived from *E. coli*'s (PQ795799.1) 16S rRNA gene sequence and other reference sequences.



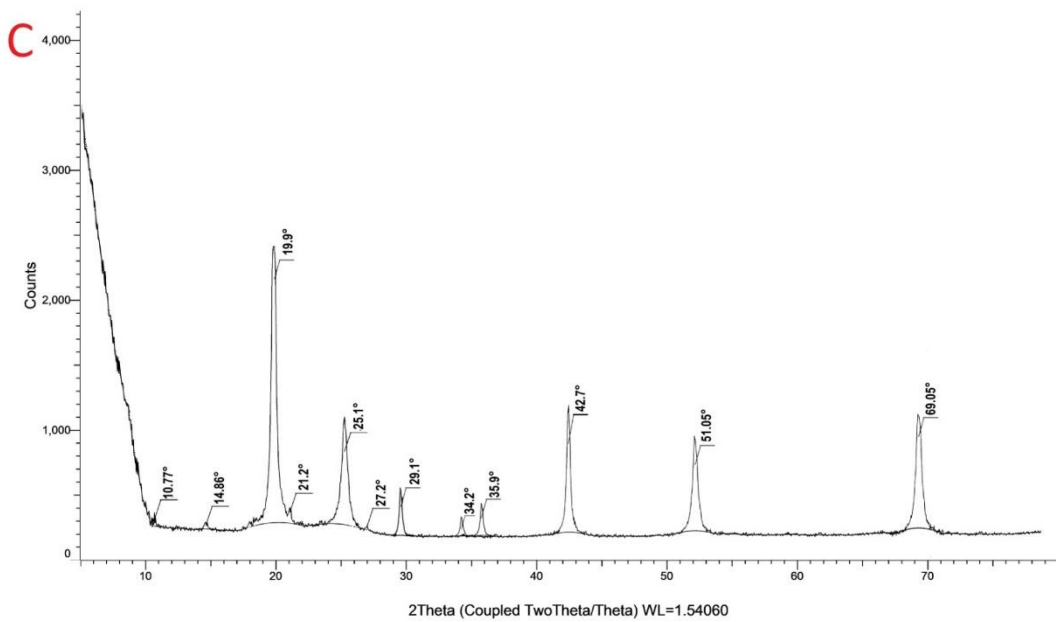


Figure. 3 Phytofabricated MS-ZVI@PP characterization a) UV-visible spectrum; b) FTIR spectra; c) MS-ZVI@PP XRD pattern.

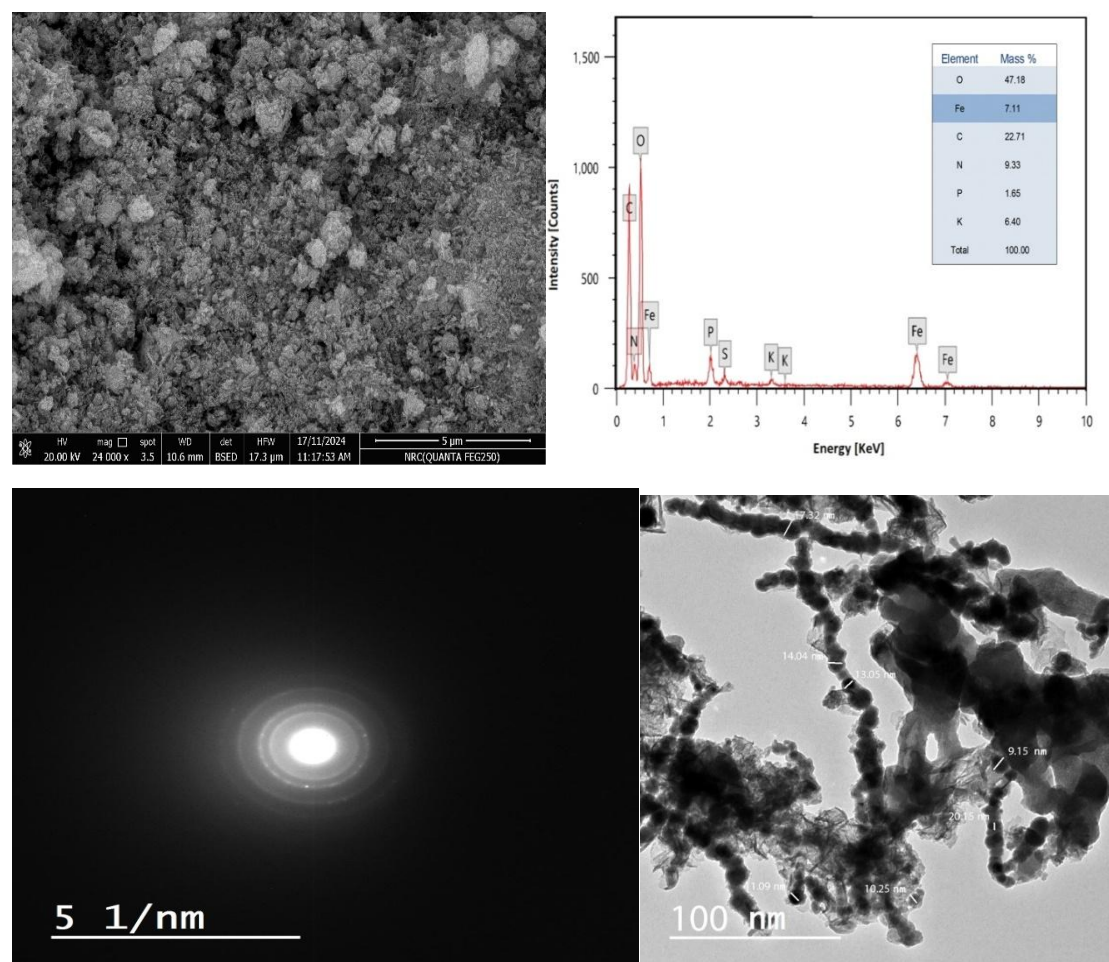


Figure. 4 Plant-based MS-ZVI@PP morphological characterization: a) SEM pictures magnified by 5 μm ; b) EDX analysis; c & d) TEM images.

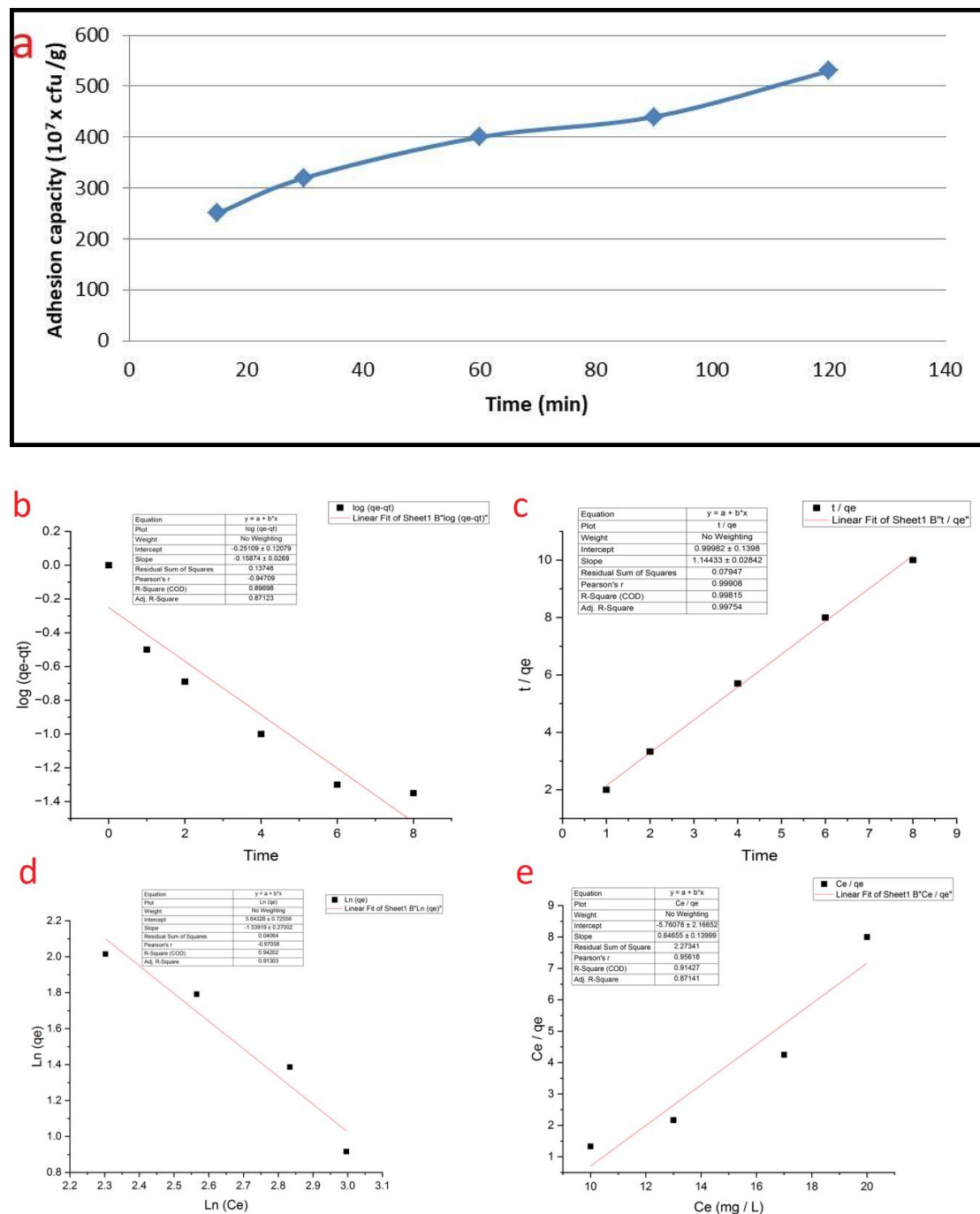
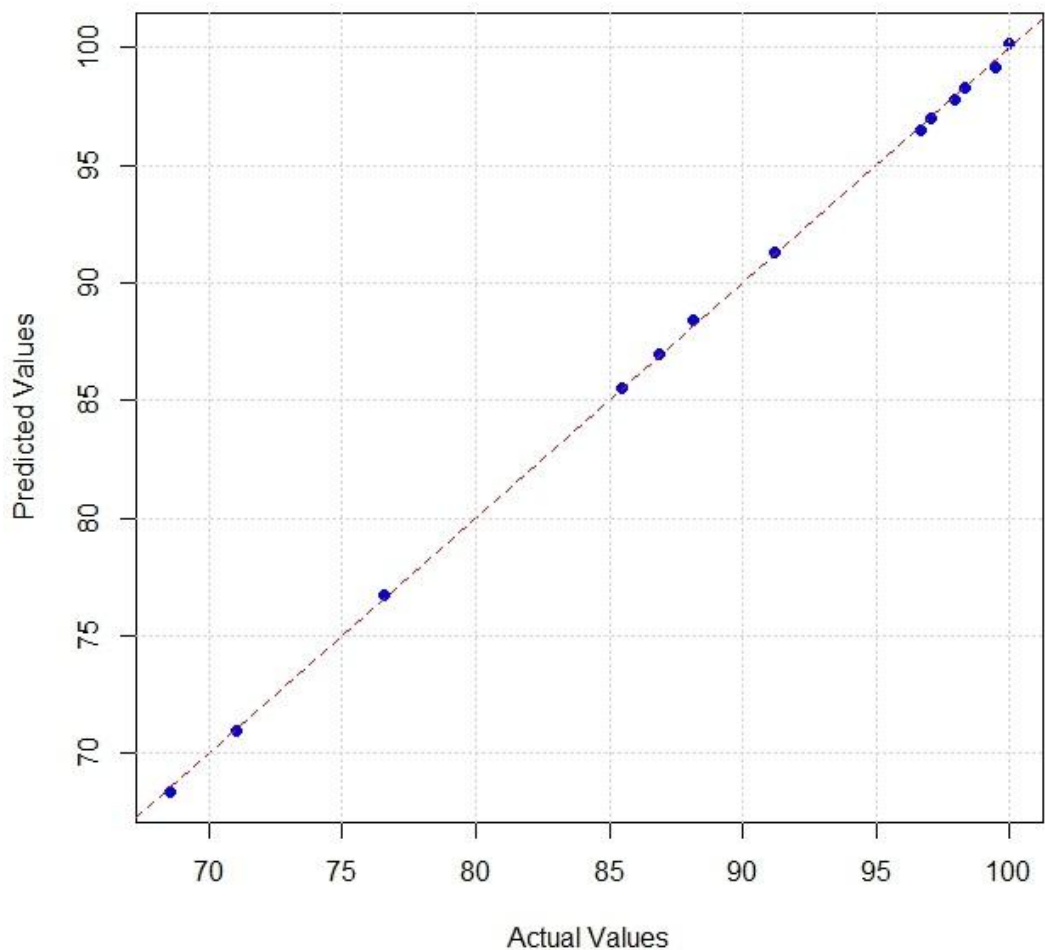


Figure. 5 Plots of kinetic and isothermal models that describe the adherence of *E. coli*-PQ795799.1 onto MS-ZVI@PP. Adhesion capacity (a); Freundlich isotherm Langmuir isotherm; pseudo-first-order model (b); pseudo-second-order model (c); and Langmuir isotherm (e).

a**Predicted vs Actual Values**

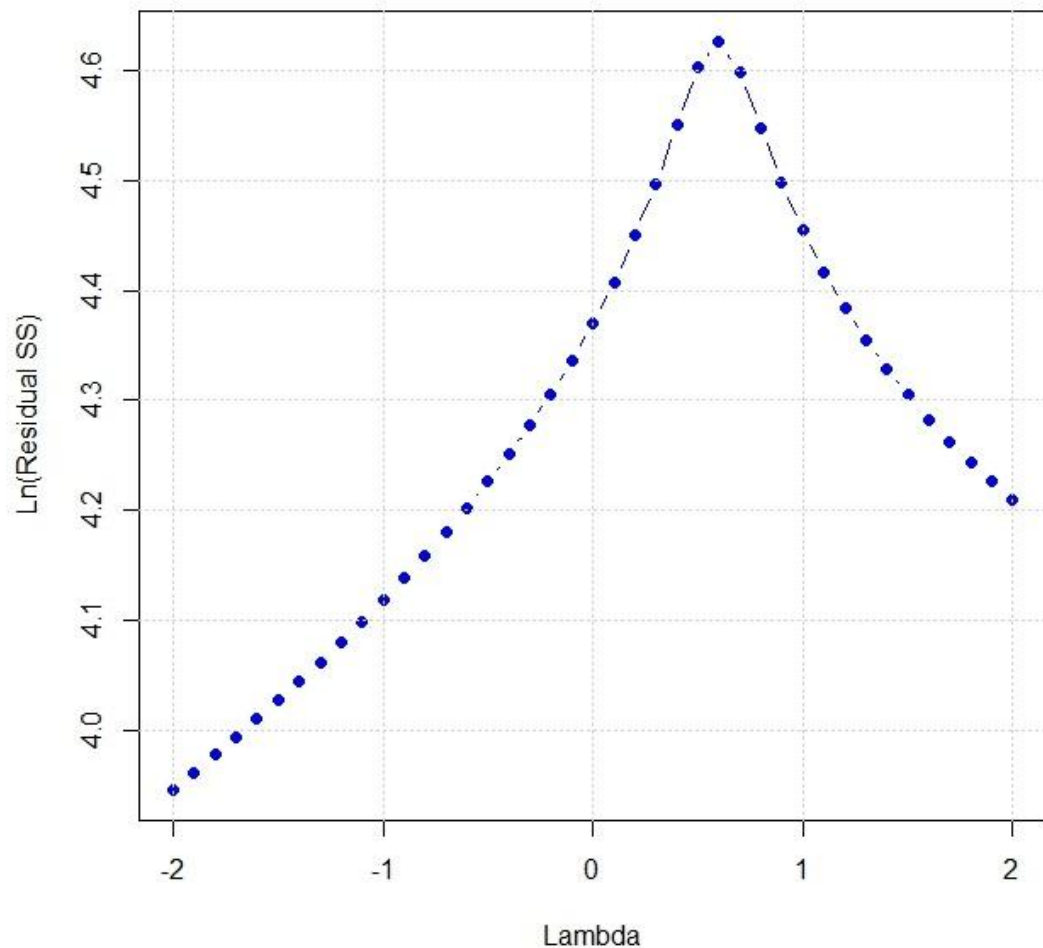
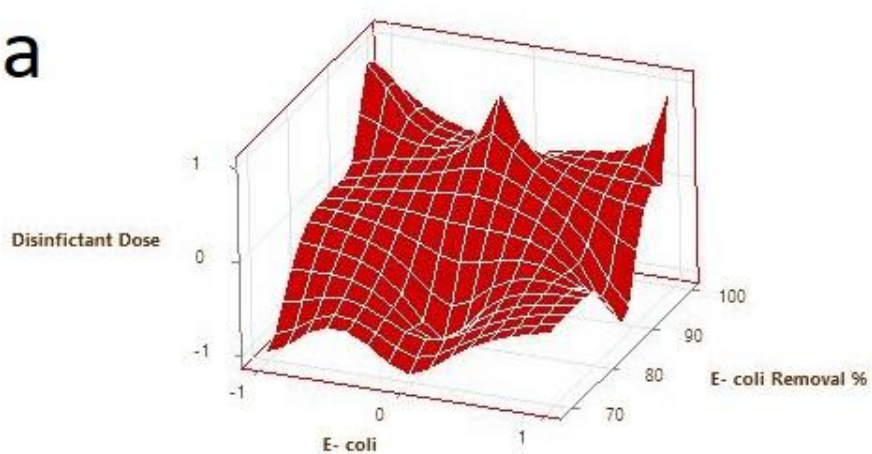
b**Ln(Residual SS) vs Lambda**

Figure. 6 Plot of expected versus real values of *E. coli* elimination by Ms-nZVI@pp
(a) and (b) Box–Cox plot of model transformation

a

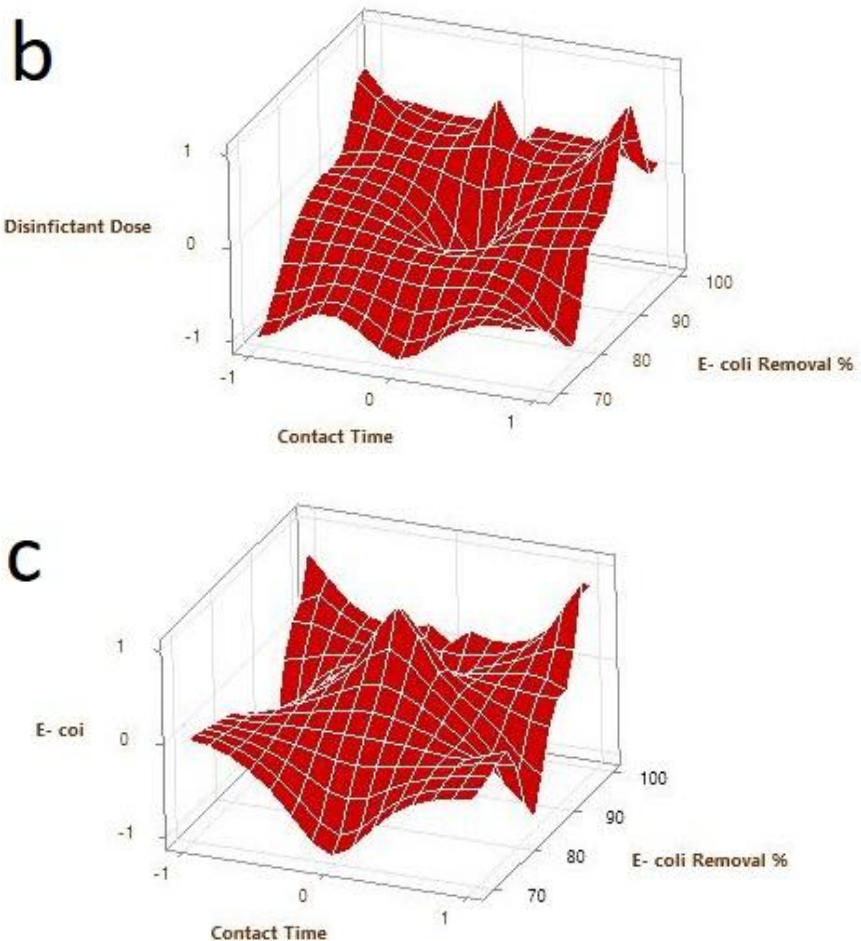


Figure. 7 Response surface plots showing *E. coli*- PQ795799.1 removal efficiency (%) vs. (a) contact time and disinfectant dose, (b) *E. coli* concentration and disinfectant dose, and (c) contact time and *E. coli* concentration

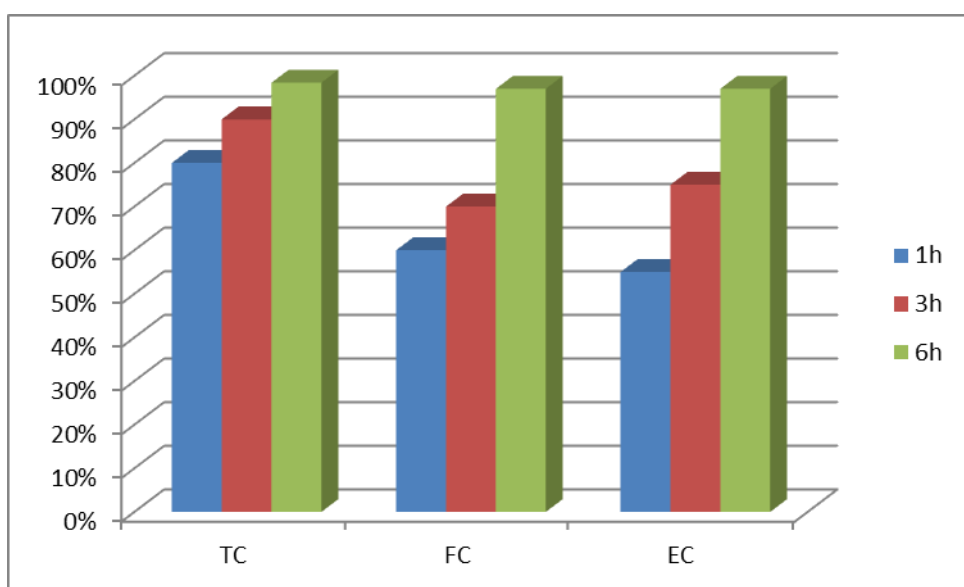


Figure. 8 Bacteria removal efficiency concerning contact time of immobilized phytofabricated MS-ZVI@PP. The mean \pm SE of three duplicate tests is used to express the data, and columns with different letters denote significant differences at p.

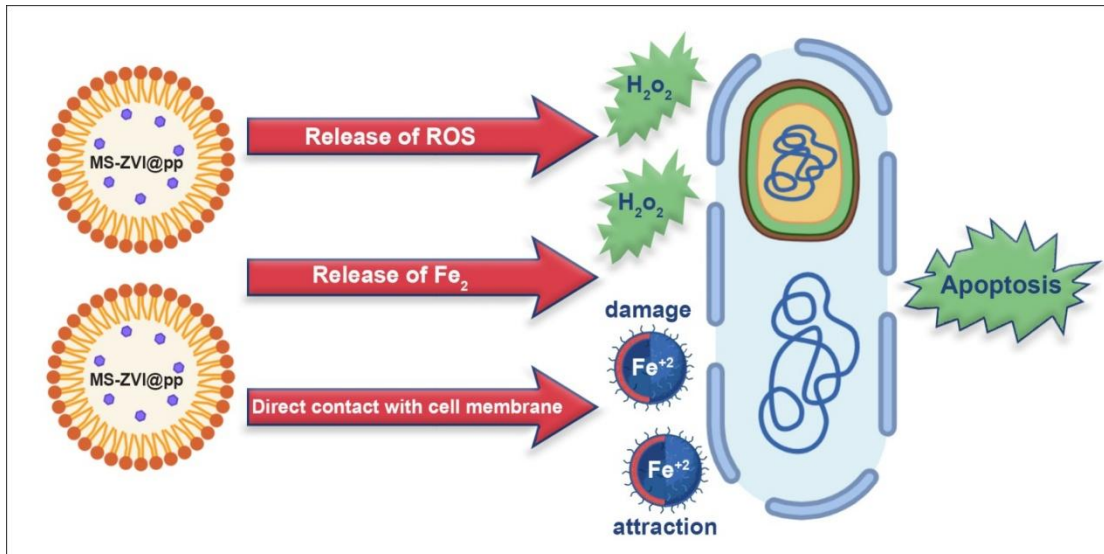


Figure 9 Disinfection mechanism of phytofabricated MS-ZVI@PP